Nephrol Dial Transplant (2018) 1–11
doi: 10.1093/ndt/gfy080

ndt
Nephrology Dialysis Transplantation

ORIGINAL ARTICLE

The 6-hydroxychromanol derivative SUL-109 ameliorates renal injury after deep hypothermia and rewarming in rats

Pieter C. Vogelaar[1,2], Maurits Roorda[1], Edwin L. de Vrij[1], Martin C. Houwertjes[3], Maaike Goris[1], Hjalmar Bouma[1,4], Adrianus C. van der Graaf[2], Guido Krenning[2,5,*] and Robert H. Henning[1,*]

[1]Department of Clinical Pharmacy and Pharmacology, University Medical Center Groningen, University of Groningen, Groningen, The Netherlands, [2]Sulfateq B.V., Groningen, The Netherlands, [3]Department of Anesthesiology, University Medical Center Groningen, University of Groningen, Groningen, The Netherlands, [4]Department of Internal Medicine, University Medical Center Groningen, University of Groningen, Groningen, The Netherlands and [5]Cardiovascular Regenerative Medicine, Department of Pathology and Medical Biology, University Medical Center Groningen, University of Groningen, Groningen, The Netherlands

Correspondence and offprint requests to: Guido Krenning; E-mail: g.krenning@umcg.nl; Twitter handle: @cavarem_umcg @pcvogel
*These authors contributed equally to this work.

ABSTRACT

Background. Mitochondrial dysfunction plays an important role in kidney damage in various pathologies, including acute and chronic kidney injury and diabetic nephropathy. In addition to the well-studied ischaemia/reperfusion (I/R) injury, hypothermia/rewarming (H/R) also inflicts acute kidney injury. Substituted 6-hydroxychromanols are a novel class of mitochondrial medicines that ameliorate mitochondrial oxidative stress and protect the mitochondrial network. To identify a novel 6-hydroxychromanol that protects mitochondrial structure and function in the kidney during H/R, we screened multiple compounds *in vitro* and subsequently assessed the efficacy of the 6-hydroxychromanol derivatives SUL-109 and SUL-121 *in vivo* to protect against kidney injury after H/R in rats.

Methods. Human proximal tubule cell viability was assessed following exposure to H/R for 48/4 h in the presence of various 6-hydroxychromanols. Selected compounds (SUL-109, SUL-121) or vehicle were administered to ketamine-anaesthetized male Wistar rats (IV 135 µg/kg/h) undergoing H/R at 15°C for 3 h followed by rewarming and normothermia for 1 h. Metabolic parameters and body temperature were measured throughout. In addition, renal function, renal injury, histopathology and mitochondrial fitness were assessed.

Results. H/R injury *in vitro* lowered cell viability by 94 ± 1%, which was counteracted dose-dependently by multiple 6-hydroxychomanols derivatives. *In vivo*, H/R in rats showed kidney injury molecule 1 expression in the kidney and tubular dilation, accompanied by double-strand DNA breaks and protein nitrosylation. SUL-109 and SUL-121 ameliorated tubular kidney damage, preserved mitochondrial mass and maintained cortical adenosine 5′-triphosphate (ATP) levels, although SUL-121 did not reduce protein nitrosylation.

Conclusions. The substituted 6-hydroxychromanols SUL-109 and SUL-121 ameliorate kidney injury during *in vivo* H/R by preserving mitochondrial mass, function and ATP levels. In addition, both 6-hydroxychromanols limit DNA damage, but only SUL-109 also prevented protein nitrosylation in tubular cells. Therefore SUL-109 offers a promising therapeutic strategy to preserve kidney mitochondrial function.

Keywords: 6-hydroxychromanol, hypothermia/rewarming, mitochondria, renal injury, tubular cells

INTRODUCTION

Mitochondrial dysfunction plays a key role in the aetiology of certain types of acute and chronic kidney injury, including diabetic nephropathy [1–3]. The kidney has a high energy demand [1] and within the organ the proximal tubule compartment is particularly metabolically active. It contains the largest amount of mitochondria [4]. The kidney depends on mitochondrial oxidative phosphorylation (OXPHOS) to perform tubular reabsorption. In comparison with their distal counterparts, proximal tubules are incapable of synthesizing glutathione [5] and are characterized by high mitochondrial membrane potential and large mitochondrial membrane potential fluctuations [6]. These characteristics make the proximal tubule vulnerable to disruptions in the mitochondrial network that occur during hypoxia and adenosine 5′-triphosphate (ATP) depletion [7]. These data suggest that prevention of mitochondrial dysfunction offers a distinct therapeutic target for the prevention of kidney disease [8].

Hypothermia/rewarming (H/R) offers a model in which the contribution of mitochondrial dysfunction to renal disease can be studied in an acute setting. During *in vivo* hypothermia, a decrease in the metabolic rate mitigates the deleterious effects of

hypoxia [9, 10], similar to the adaptive changes that occur in the kidney during ischaemia/reperfusion (I/R) or sepsis-induced acute kidney injury [11]. Upon rewarming, oxygen demand increases rapidly while supply is lagging, resulting in the depletion of ATP stores [12] and a surge in the production of mitochondrial-derived reactive oxygen species (ROS) and reactive nitrogen species (RNS). Moreover, H/R impairs neutralization of products of oxidative stress due to decreased superoxide dismutase enzyme activity and a reduction in glutathione peroxidase substrate levels [13]. The imbalance of increased ROS/RNS production and the decrease in antioxidant defence results in excess oxidative and nitrosative stress, which facilitates lipid peroxidation, oxidation and nitrosylation of proteins and oxidative damage to DNA. Moreover, the oxidative damage to mitochondria causes a disruption in calcium homeostasis and subsequent cytochrome C release [14], ultimately leading to the induction of apoptosis in renal tubular cells [15] and acute tubular cell necrosis [16].

Prevention of kidney disease by administering antioxidants such as α-tocopherol has proven effective in rats in several studies [17, 18], although only at high concentrations or for several days prior to the insult. TROLOX, a molecule that contains the antioxidant moiety of α-tocopherol with better water solubility (logS), offers protection from I/R kidney injury in rats but, similar to α-tocopherol, high concentrations of 12 mg/kg/h TROLOX are required [19]. Moreover, while effective at high doses in experimental studies, antioxidant therapy to prevent acute kidney injury in humans has been ineffective [20, 21].

An alternative approach to prevent kidney disease is to address the underlying mitochondrial dysfunction. The rapid depletion of tubular ATP stores during I/R and H/R suggests that consolidation of OXPHOS might have beneficial effects, besides reducing oxidative stress. We hypothesize that compounds that maintain mitochondrial homeostasis might offer a benefit in kidney diseases associated with mitochondrial dysfunction. H/R offers a way to study early kidney injury in a model in which mitochondrial respiration is impaired by a highly standardized insult. By assessing kidney health 1 h after H/R, it is possible to identify the initial adaptations to kidney injury as well as in metabolism. This is in contrast to chronic models like diabetes or acute models such as I/R, where systemic processes like the immune response can make it difficult to discern the cause of kidney injury from secondary processes.

We recently showed that the 6-hydroxychromanol SUL-109 can improve OXPHOS while protecting cells against H/R injury [22]. To explore 6-hydroxychromanol efficacy in limiting H/R-induced kidney injury, we first screened a library of 11 compounds on human proximal tubule epithelial cells (PTECs) *in vitro*. The compounds SUL-109 and SUL-121 were selected on the basis of their similarly high potencies with different antioxidant capacities and subsequently tested for protection against H/R-induced acute kidney injury in rats.

MATERIALS AND METHODS

Compounds

A 6-hydroxychromanol library containing 11 compounds was synthesized (Syncom, Groningen, The Netherlands). Compound purity of ≥98% after recrystallization was confirmed by high-performance liquid chromatography analysis (Waters, Xbride BEH C18 XP column, 2.1 × 50 mm, 2.5 µm) and nuclear magnetic resonance (Varian, Palo Alto, CA, USA) spectra were in accordance with chemical structure (^{1}H, 300 MHz, solvent *d*-MeOD). Solubility (ClogP) was calculated as *n*-octanol/water partition coefficient. Molar refractivity (MR) is the measure of total polarizability of a molecule. These characteristics, as well as the total polar surface area (tPSA), logS and the acid dissociation constant (pKa), were calculated using ChemDraw Professional 15.0 (PerkinElmer Informatics, Waltham, MA, USA).

Isolation and culture of cells

Human primary proximal tubule epithelial cells (PTECs) were obtained as previously described [23, 24]. PTECs were cultured in Dulbecco's modified Eagle's medium (Thermo Fisher Scientific, Etten-Leur, The Netherlands, catalogue no. 41965) with 10% foetal bovine serum (Thermo Fisher Scientific, catalogue no. 10270106) and 1% penicillin/streptomycin (Thermo Fisher Scientific, catalogue no. 5140122) in a humidified incubator at 37°C and 5% carbon dioxide (CO_2).

In vitro H/R protocol

PTECs were seeded on a 96-well plate. After 24 h, culture medium was replaced by pre-warmed cell culture medium containing 1×10^{-4}–5.12×10^{-11} M of 6-hydroxychromanol ($n = 6$ per concentration). After 1 h of incubation with test compounds, cells were placed in a cold room (2–8°C) for 48 h in airtight plastic bags to enclose CO_2-enriched air, followed by a 4-h rewarming period under standard culture conditions.

Neutral red uptake assay

After 2-h of rewarming, culture medium was aspirated and replaced with 150 µL cell culture medium containing 0.4 mg/mL Neutral Red (Sigma-Aldrich, Zwijndrecht, The Netherlands, catalogue no. N4638). After an additional 2-h incubation period, Neutral Red solution was aspirated and cell-trapped Neutral Red was solubilized in 100 µL solution containing 50% ethanol, 1% glacial acetic acid in distilled water (dH_2O). Absorbance was measured at a wavelength of 550 nm on a plate reader (ELx808, Biotek, Winooski, VT, USA). The 550 nm optical density (OD_{550}) of Neutral Red was used as a readout for the number of viable cells.

TROLOX-equivalent antioxidant capacity

A solution of 7 mM 2,2′-azino-bis(3-ethylbenzothiazoline-6-sulphonic acid) [ABTS; Chemical Abstract Service (CAS) no. 30931-67-0] and 2.45 mM potassium persulfate ($K_2S_2O_8$; CAS no. 7727-21-1) was incubated overnight at room temperature to enable the formation of ABTS-● radical cations to obtain a solution with an OD750 of ≥ 0.7 (+0.05). To each well, 200 µL of ABTS-● solution was added, after which 6-hydroxychromanols were added at final concentrations of 1×10^{-3} down to 1.6×10^{-5} M. Subsequently the plate was incubated for 25 min at room temperature on an orbital shaker at 120 rpm, after which the OD_{750} was measured on a plate reader (ELx808, Biotek).

TROLOX-equivalent antioxidant capacity (TEAC) was expressed as the amount of decolourization ($\Delta OD_{705}/\mu M$) of a compound over that of an equal concentration of TROLOX.

Animal experiments

The experimental protocol was approved by the Institutional Animal Care and Use Committee of the University of Groningen (DEC5920 and DEC6725). Male Wister rats (Charles River Laboratories, Den Bosch, The Netherlands) with a weight of 400 ± 41 g were housed as described earlier [25]. Rats were randomized to one of four experimental groups, consisting of a euthermic control (37°C) experimental group, a group that underwent forced cooling and rewarming while being administered the 6-hydroxychromanol SUL-109 or SUL-121 and the control group that underwent the same procedure while receiving vehicle ($n = 4$ per group). Forced hypothermia under anaesthesia was applied as described earlier [25]. In brief, rats were anaesthetized by isoflurane inhalation and mechanically ventilated, after which the carotid artery and jugular vein were cannulated for blood sampling and infusion of vehicle or 6-hydroxychromals, respectively. Anaesthesia was switched to intravenous infusion of ketamine (5 µg/kg/min) 60 min prior to hypothermia. Animals in the euthermic control group were also anaesthetized with ketamine but did not undergo hypothermia. SUL-109 or SUL-121 infusion was started at 135 µg/kg/h 30 min prior to cooling. Animals in the vehicle group received equal amounts of solvent (dimethyl sulphoxide). After 30 min of cooling, infusion rates of ketamine and SUL-109/-121 or vehicle were reduced by 50%. Infusion rates were restored to baseline at 30 min after the initiation of rewarming. Rats were maintained anaesthetized under normothermia for 60 min followed by euthanization under anaesthesia. Arterial heparinized blood samples were acquired immediately prior to cooling, immediately prior to rewarming and 1 h after rewarming to 37°C (Figure 3A) and at corresponding time points in the euthermic control group. Tissue samples were snap frozen in liquid nitrogen or fixed, followed by embedding in paraffin.

Histopathology

Kidney samples were fixed in zinc solution (0.1 M Tris buffer, pH 7.4 with 0.5 g calcium acetate, 5.0 g zinc acetate and 5.0 g zinc chloride) and embedded in paraffin. The thickness of the sections used for histological analyses was 5 µm. Kidney sections were oxidized in 0.5% periodic acid solution, stained with Schiff reagent and counterstained with haematoxylin. Kidney sections were scanned with a digital slide scanner (Hamamatsu Photonics, Hamamatsu, Japan) and imported into ImageJ FiJi digital image analysis software [26]. Glomerular damage was assessed by determining contraction of the glomerular tuft and shrinkage of the glomerular content in at least 100 glomeruli per rat. Tubulointerstitial damage was quantified by determining tubular dilatation and widening of the tubular lumen by particle analysis [27]. For a detailed description of this analysis, see Supplementary data, methods supplement.

Immunohistochemistry and immunofluorescence

For immunohistochemistry, 5-µm thick cryosections were incubated with antibodies against kidney injury molecule-1 (KIM-1; 15 µg/mL; R&D Systems, Abingdon, UK, catalogue no. AF3689) or 3-nitrotyrosine residues (3-NT; 10 µg/mL; Sigma-Aldrich, catalogue no. SAB5200009) at room temperature overnight. Secondary antibodies used were polyclonal horseradish peroxidase (HRP)-linked rabbit anti-mouse immunoglobulin G (IgG) and polyclonal rabbit anti-goat IgG (5 µg/mL; Santa Cruz Biotechnology, Huissen, The Netherlands, catalogue nos. sc-358917 and sc-2768). Sections were developed using 3-amino-9-ethylcarbazole high-sensitivity substrate chromogen. Sections were mounted in Faramount (Dako, Heverlee, Belgium) aqueous mounting medium. For immunofluorescence, 5-µm thick cryosections of the kidney were fixed with 3.7% formaldehyde and 0.1% Triton X-100 in phosphate-buffered saline. Sections were stained using antibodies against 53bp1 (2 µg/mL; Santa Cruz Biotechnology, catalogue no. sc-22760) and γ-H2AX (2 µg/mL; Merck, Schiphol-Rijk, The Netherlands, catalogue no. 05-636) or Tom20 (2 µg/mL; Santa Cruz Biotechnology, catalogue no. sc-11415). Secondary antibodies consisted of fluorescein isothiocyanate–conjugated polyclonal goat anti-rabbit IgG (10 µg/mL; Thermo Fisher Scientific, catalogue no. F-2765) and goat–anti-mouse IgG TRITC-conjugated polyclonal antibody (5 µg/mL; Sanbio, Uden, The Netherlands, catalogue no. 130-03). Nuclei were visualized with 4′,6-diamidino-2-phenylindole (DAPI; 0.25 µg/mL; Sigma-Aldrich, catalogue no. D9542) and digital images were captured with an InCell Analyzer 2200 (GE Healthcare, Chalfont St Giles, UK). For a detailed description of image analysis, see Supplementary data, methods supplement.

Western blotting

Frozen kidney tissue samples (∼50 mg) were homogenized in 0.4 mL of RIPA buffer containing a protease inhibitor cocktail (Roche cOmplete, Sigma-Aldrich, catalogue no. 11697498001) and soluble protein concentrations were determined using a Bradford protein assay. 5X loading buffer (4% sodium dodecyl sulfate, 10% 2-mercaptoethanol, 20% glycerol, 0.004% bromophenol blue, 0.125 M Tris-HCl, pH = 6.8) was added to protein lysates to 1X, after which they were stored at −20°C until use. Forty micrograms of protein per lane were separated on 4–20% sodium dodecyl sulfate–polyacrylamide gradient gels (Thermo Fisher Scientific, catalogue no. 25204). Proteins were blotted onto nitrocellulose membranes (Bio-Rad Laboratories, Munich, Germany) and incubated overnight at 4°C with the primary antibodies in 3% bovine serum albumin/tris-buffered saline with KIM-1 (0.1 µg/mL; R&D Systems, Abingdon, UK, catalogue no. AF3689) or 3-NT (1 µg/mL; Sigma-Aldrich, catalogue no. SAB5200009B3). Subsequently membranes were incubated with 0.08 µg/mL of either HRP-linked goat anti-rabbit (Santa Cruz Biotechnology, catalogue no. sc-2030), rabbit anti-goat (Santa Cruz Biotechnology, catalogue no. sc-2768) or rabbit anti-mouse IgG secondary antibody (Santa Cruz Biotechnology, catalogue no. sc-358917). Blots were then developed using the SuperSignal West Dura Extended Duration Substrate (Thermo Fisher Scientific)

according to the manufacturer's protocol. Protein bands were visualized using a GeneGnome device (Westburg, Leusden, The Netherlands) and band intensities were quantified using Totallab (Newcastle upon Tyne, UK). α-Tubulin was used as a reference protein to normalize protein concentrations.

Biomarker levels

Plasma creatinine, high-sensitivity troponin T, aspartate transaminase (ASAT) and alanine transaminase (ALAT) levels were determined by the University Medical Center Groningen Department of Laboratory Medicine using standardized protocols on a modular analyser (Roche, Almere, The Netherlands).

ATP measurements

To measure ATP levels in rat kidneys, a modified protocol to isolate ATP was used [28]. In short, sections of frozen kidneys were cut and homogenized in 500 µL of ice-cold TE-saturated phenol (Sigma-Aldrich, catalogue no. 77607) using a motorized pellet pestle tissue grinder for 30 s on ice. Ice-cold chloroform (100 µL) and dH_2O (75 µL) were added and samples were shaken vigorously for 20 s. Then samples were centrifuged at 10 000 *g* at 4°C for 5 min and 10 µL of the dH_2O supernatant was resuspended into 990 µL of ice-cold dH_2O. ATP concentrations were measured using a firefly-based luminescence kit (Promega, Madison, WI, USA, catalogue no. FF2000) in a microplate reader (Synergy H4, Biotek) according to the manufacturer's instructions. Measurements were corrected for the amount of protein (Bradford protein assay) and interpolated using a 1×10^{-7}–1×10^{-10} M ATP standard curve.

Statistical analysis and data presentation

Data were confirmed to be in Gaussian distribution (D'Agostino–Pearson test). Outliers were identified using a ROUT analysis and excluded from the analysis [29]. All variables are expressed as mean ± SD. Differences between groups were tested for significance using a Student's *t*-test or repeated-measures analysis of variance (ANOVA) (Tukey honest significant difference post-hoc testing). Differences in TEAC values between 6-hydroxychromanols were tested for significance using a one-way ANOVA with Bonferroni post-hoc analysis. P-values <0.05 were considered statistically significant (Graphpad Prism 6.0, GraphPad Software, La Jolla, CA, USA).

RESULTS

6-Hydroxychromanols maintain cell viability after H/R

H/R (48/8 h) resulted in a 94 ± 1% loss of viability of PTECs (Figure 1A). 6-Hydroxychromanols maintained cell viability in PTECs with varying efficacies (Table 1). The addition of a piperazine side group (Figure 1B) to TROLOX, rendering the compound SUL-109, resulted in a 59-fold increase in potency compared with TROLOX by decreasing the half maximal effective concentration (EC_{50}) from 5.2 µM to 87.9 nM (Figure 1A; $P < 0.001$, extra sum-of-squares F-test). The addition of a 1-(2-hydroxyethyl)piperazine side group to TROLOX, yielding the compound SUL-121, resulted in a 382-fold increase in potency with an EC_{50} of 13.6 nM (Table 1; $P < 0.001$, extra sum-of-squares F-test).

We examined whether the physiochemical properties of 6-hydroxychromanols correlated with their potency. These characteristics are used to predict the efficacy and potency of small molecules based on their solubility, membrane passage and the ability to engage in receptor binding. Lipophilicity correlated negatively with EC_{50} ($P < 0.05$, $R^2 = 0.50$; Figure 2A), whereas tPSA correlated positively with EC_{50} ($P < 0.05$, $R^2 = 0.37$; Figure 2B). Notably, EC_{50} did not correlate with antioxidant capacity (TEAC values) ($P > 0.05$, $R^2 = 0.12$; Figure 2C) nor was a correlation found between EC_{50} and MR (Figure 2D). Lastly, both solubility (Figure 2E) and pKa (Figure 2F) were unrelated to compound potency.

To obtain proof of concept of the protection of the kidney by substituted 6-hydroxychromanols *in vivo*, SUL-109 and SUL-121 were administered throughout in anaesthetized rats undergoing cooling to a core body temperature of 15.2 ± 0.2°C for 3 h, followed by rewarming and 1 h stabilization at 37°C.

Haemodynamics, blood cell counts and blood gases in H/R were unaffected by 6-hydroxychromanols

Whole-body forced hypothermia to 15°C (Figure 3A) decreased heart rate to ∼18% of normothermic baseline values ($P < 0.01$; Table 2) and reduced mean arterial pressure to ∼41% of normothermic baseline values ($P < 0.01$). Haemodynamics throughout the experiment were unaffected by SUL-109 (Table 2) and SUL-121 (Supplementary data, Table S1). Hypothermia reduced the white blood cell (WBC) count to ∼40% ($P < 0.05$) of pre-hypothermia. SUL-109 augmented the hypothermia-induced reduction of WBC count (∼18% of pre-hypothermia; $P < 0.001$; Table 2), whereas the WBC count was unaffected by SUL-121 (Supplementary data, Table S1). Hypothermia also caused a decrease in blood platelet count by ∼30% ($P > 0.05$ versus pre-hypothermia), which was unaffected by SUL-109 and SUL-121 (Table 2 and Supplementary data, Table S1). In all animals, WBC and platelet counts returned to pre-hypothermia values after rewarming. In all SUL-treated groups, the partial pressure of oxygen (pO_2) did not change throughout the experiment (Table 2 and Supplementary data, Table S1). The partial pressure of CO (pCO_2) decreased by ∼23% ($P < 0.001$) in the H/R vehicle group, whereas pCO_2 values in SUL-109 animals decreased by 50% ($P < 0.001$ compared with vehicle). pCO_2 levels during hypothermia were unaffected by SUL-121. Post-hypothermia, pCO_2 in the H/R vehicle group, SUL-109 group and SUL-121 group fully recovered to pre-hypothermia values. During hypothermia, plasma glucose and lactate levels increased ∼3.7-fold and ∼2.3-fold, respectively, which were unaffected by administration of SUL-109 and SUL-121.

Plasma and serum markers for renal, cardiomuscular or hepatic injury were unaffected by 6-hydroxychromanols

To assess kidney function, plasma creatinine levels were measured at euthanization (Table 2 and Supplementary data, Table S1). In euthermic control animals, the plasma creatinine level was 21.0 ± 2.6 µM, which increased to 50.3 ± 3.3 µM by

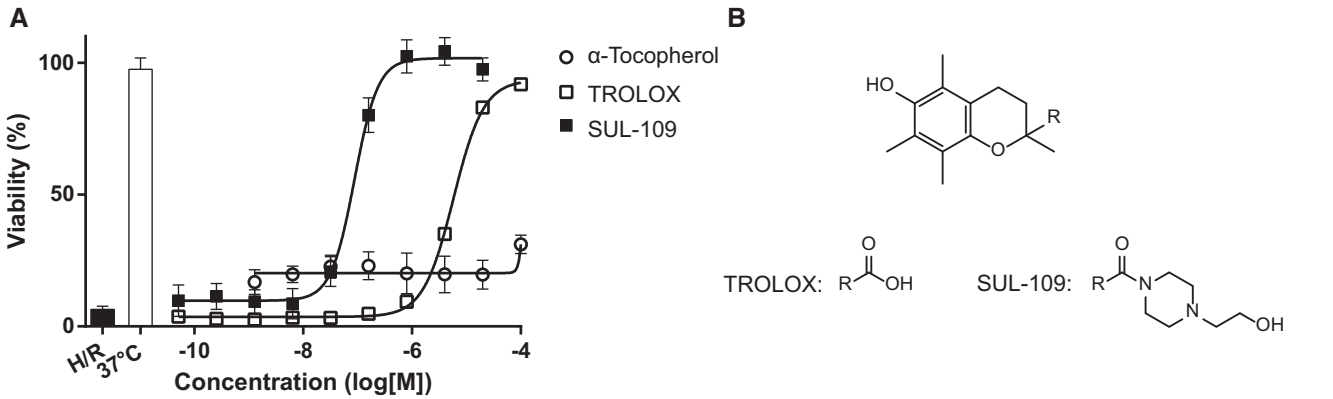

FIGURE 1: (**A**) 6-Hydroxychromanols protect the viability of PTECs after 48 h of storage at 2–8°C. Data are representative of at least three replicate experiments and are shown as mean ± SD ($n = 6$) and curve-fitted to a four-parameter non-linear regression. (**B**) Molecular structure of the compounds used in this study. H/R, positive control H/R cells; 37°C, negative control normothermia cells.

Table 1. The physiochemical properties and *in vitro* efficacy of the compounds in the library of 6-hydroxychromanol derivatives

Chromanol	MW (Da)	ClogP	MR (cm^3/mol)	tPSA (Å^2)	logS	pKa	EC_{50} (M)	TEAC (a.u.)
TROLOX	250.29	3.01	70.60	66.76	−2.56	9.91	$5.81 \times 10^{-6} \pm 1.52 \times 10^{-7}$	1.00 ± 0.05
α-Tocopherol	430.72	9.98	139.21	29.46	−8.15	10.16	$>1 \times 10^{-4}$	n.d.
SUL-95	319.4	2.84	92.04	59.00	−2.58	9.92	$1.52 \times 10^{-6} \pm 5.42 \times 10^{-8}$	1.04 ± 0.10
SUL-109	362.47	2.25	105.35	73.24	−2.32	9.92	$8.79 \times 10^{-8} \pm 6.32 \times 10^{-9}$	0.76 ± 0.06
SUL-121	354.82	2.60	94.14	61.80	−2.60	9.92	$1.36 \times 10^{-8} \pm 1.39 \times 10^{-9}$	0.86 ± 0.13
SUL-122	406.52	2.60	116.27	82.47	−2.22	9.92	$5.19 \times 10^{-7} \pm 2.88 \times 10^{-8}$	0.35* ± 0.02
SUL-125	265.30	2.91	74.40	78.79	−2.38	9.94	$3.39 \times 10^{-7} \pm 2.25 \times 10^{-8}$	0.97 ± 0.03
SUL-128	355.90	4.06	96.32	52.93	−3.15	10.12	$2.12 \times 10^{-8} \pm 9.38 \times 10^{-10}$	1.12 ± 0.07
SUL-134	333.42	3.05	96.38	70.00	−2.84	9.92	$2.97 \times 10^{-7} \pm 3.11 \times 10^{-8}$	0.93 ± 0.03
SUL-135	333.42	3.05	96.38	70.00	−2.84	9.92	$2.60 \times 10^{-6} \pm 2.49 \times 10^{-7}$	0.57* ± 0.05
SUL-137	410.99	3.57	112.90	61.80	−4.09	9.98	$6.68 \times 10^{-7} \pm 2.27 \times 10^{-8}$	0.23* ± 0.01
SUL-141	376.46	0.04	105.30	90.31	−2.58	9.92	$1.25 \times 10^{-5} \pm 9.26 \times 10^{-7}$	1.55 ± 0.08
SUL-142	376.46	0.04	105.30	90.31	−2.58	9.92	$1.96 \times 10^{-5} \pm 2.32 \times 10^{-6}$	1.53 ± 0.07

Data are presented as mean ± SD of at least three replicate experiments.
ClogP, calculated solubility; EC_{50}, concentration at which 50% viability of PTECs was observed after 48 h of H/R; MW, molecular weight.
*$P < 0.05$ versus TROLOX, one-way ANOVA.

H/R in the vehicle group, a change that was unaffected by SUL-109 (45.0 ± 11.0 μM) and SUL-121 (37.8 ± 8.0 μM). Cardiac injury was determined by measuring levels of troponin T. In euthermic control animals, troponin T levels of 1017 ± 129 ng/mL were observed. The post-hypothermia plasma level in the vehicle group showed an increase to 7408 ± 1930 ng/L ($P < 0.01$), which was unaffected by SUL-109 (8058 ± 3603 ng/L; Table 2) and SUL-121 (4920 ± 3261 U/L; Supplementary data, Table S1). Hepatic injury markers ASAT and ALAT in euthermic control animals were 66.2 ± 4.8 U/L and 34.4 ± 4.0 U/L, respectively. In the H/R vehicle group, these values increased to 274.3 ± 19.3 U/L and 141.5 ± 35.3 U/L, respectively ($P < 0.01$; Table 2). Neither SUL-109 nor SUL-121 affected the increase in levels of ASAT and ALAT (SUL-109: 328.8 ± 120.9 and 187.8 ± 44.1 U/L, respectively; SUL-121: 218.5 ± 53.7 and 144.5 ± 38.6 U/L, respectively).

6-Hydroxychromanols prevent H/R-induced tubular damage

In the euthermic control group, the glomerular capsule surface area was 9848 ± 556 μm^2, of which 76 ± 3% was occupied by the glomerulus. H/R in the vehicle group did not cause any changes in glomerular size, as indicated by an average glomerular capsule surface area of 9761 ± 850 μm^2 (Figure 3C), of which 69 ± 5% was occupied by the glomerulus (Figure 3C). Similarly, treatment with SUL-109 did not affect the capsule area (10 839 ± 2124 μm^2) or glomerular occupancy (70 ± 7%), nor did treatment with SUL-121 (capsule area 10 901 ± 2215 μm^2, occupied for 70 ± 6% by the glomerulus; Figure 3C, and Supplementary data, Figure S1A).

In euthermic control animals, the tubular lumen area averaged 699 ± 63 μm^2. In the vehicle group, H/R caused an increase in the tubular lumen area to 1294 ± 167 μm^2 ($P < 0.01$; Figure 3C). This increase was partially prevented in SUL-109-treated animals (lumen area 919 ± 114 μm^2; $P < 0.05$; Figure 3C) and SUL-121 (lumen area 793 ± 108 μm^2; $P < 0.05$; Supplementary data, Figure S1A), indicating both 6-hydroxychromanols reduce tubular dilatation.

Basal tubular KIM-1 expression levels in euthermic control animals were 0.17 ± 0.08. After H/R, KIM-1 abundance increased in the cortical tubuli in kidneys of vehicle-group animals to 0.54 ± 0.15 (Figure 3D), which was reduced upon SUL-109 treatment (0.23 ± 0.14; $P < 0.05$; Figure 3D) and reduced by SUL-121 treatment (0.16 ± 0.19; $P < 0.05$; Supplementary data, Figure S1B).

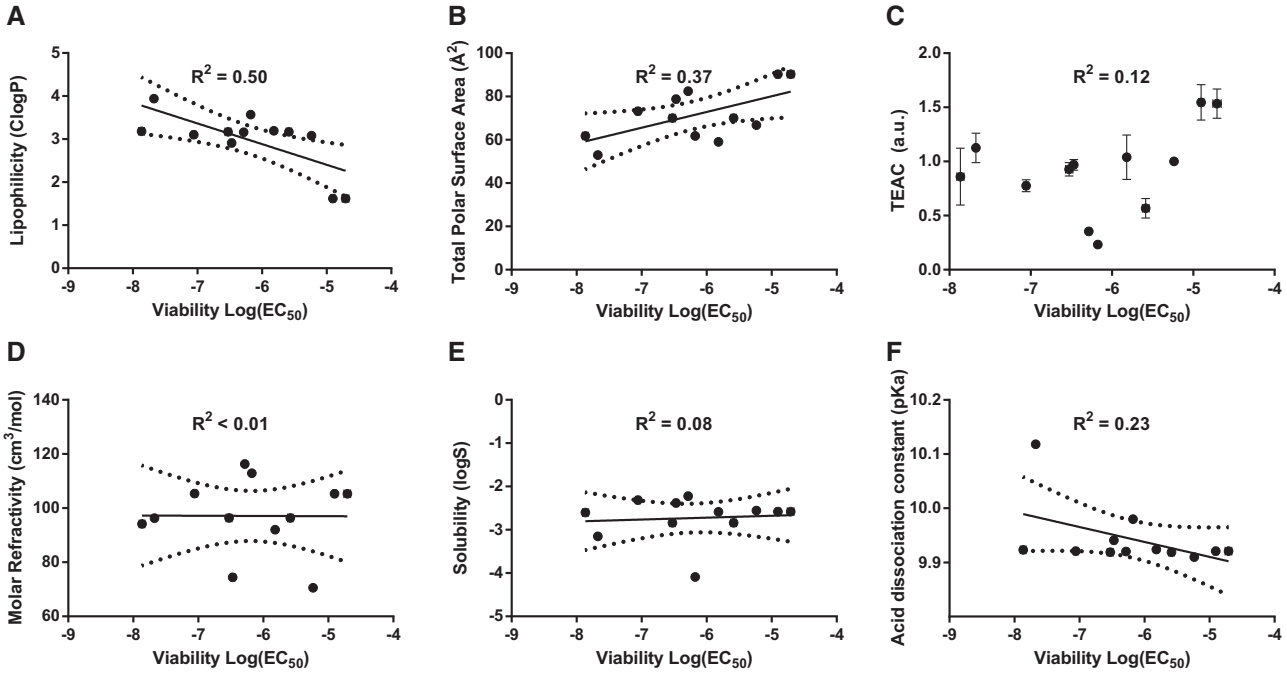

FIGURE 2: Calculated values such as (**A**) lipophilicity (ClogP) and (**B**) tPSA showed a weak correlation to EC_{50} values. (**C**) TEAC, calculated from three replicate experiments and shown as mean ± SD, did not correlate with EC_{50}. (**D**) MR, (**E**) logS and (**F**) pKa showed no relation to EC_{50} values of these chromanols.

Table 2. Plasma injury markers, blood differentials, blood gas analysis and physiological readouts during and after H/R in rats

	Euthermic	Hypothermia—vehicle			Hypothermia—SUL-109		
Markers	Post-procedure	Pre-hypothermia	Hypothermia	Post-hypothermia	Pre-hypothermia	Hypothermia	Post-hypothermia
Plasma injury markers							
Creatinine (μM)	21.0 ± 2.6			50.3* ± 3.3			45.0 ± 11.0
Troponin T (ng/L)	1017 ± 129			7408* ± 1930			8058 ± 3603
ASAT (U/L)	66.2 ± 4.8			274.3* ± 19.3			328.8 ± 120.4
ALAT (U/L)	34.4 ± 4.0			141.5* ± 35.3			187.8 ± 44.1
Blood differentials							
WBC ($\times 10^9$ L^{-1})	5.1 ± 1.0	3.6 ± 1.0	2.2 ± 2.8	5.0 ± 3.8	6.3 ± 1.7	1.1 ± 0.9#	4.6 ± 0.4
PLT	590 ± 51	703 ± 89	499 ± 114	920 ± 113	1020 ± 126	588 ± 116	1140 ± 194
Blood gas analysis							
pO_2 (kPa)	22.4 ± 1.5	16.8 ± 3.4	27.9 ± 4.0	21.9 ± 2.4	18.1 ± 1.8	27.6 ± 3.0	21.4 ± 1.9
pCO_2 (kPa)	2.8 ± 0.4	5.7 ± 0.6	4.3 ± 1.1	4.7 ± 0.7	4.5 ± 1.0	2.2 ± 0.7#	5.2 ± 1.1
Glucose (mM)	6.7 ± 0.5	5.6 ± 0.4	20.7 ± 2.4	n.d.	6.1 ± 0.6	23.1 ± 1.7	18.7 ± 1.6
Lactate (mM)	3.0 ± 0.4	2.0 ± 0.6	4.5 ± 1.9	n.d.	2.4 ± 0.6	8.7 ± 2.0	5.7 ± 2.3
Physiological parameters							
Heart rate	286 ± 28	343 ± 40	63.5 ± 12	385 ± 55	325 ± 73	51.3 ± 7	414 ± 43
MAP	77.6 ± 3.7	80.0 ± 6.4	32.6 ± 2.8	63.4 ± 6.6	101.0 ± 21.8	26.0 ± 5.3	70.3 ± 20.9

Data are presented as mean ± SD ($n = 4$ for the vehicle and SUL-109 group, $n = 6$ for the euthermic control group).
*$P < 0.01$ versus euthermic, ordinary one-way ANOVA; #$P < 0.01$ versus same time point of Hypothermia—vehicle, repeated-measures ANOVA.

6-Hydroxychromanols improve mitochondrial mass and ATP levels, ameliorate oxidative stress and inhibit DNA damage after hypothermia and rewarming

To explore changes in mitochondrial distribution and function, expression of the mitochondrial import receptor subunit Tom20 (Figure 4A) and ATP levels were measured in the cortical area of the kidney. For Tom20, the integrated density ratio of Tom20 over DAPI nuclear fluorescence was calculated (from now on Tom20/DAPI). Tom20/DAPI in the euthermic control group was 5.2 ± 0.3. In the H/R vehicle group, Tom20/DAPI decreased to 1.5 ± 0.5 ($P < 0.01$), signifying a loss of mitochondrial mass. SUL-109 partially prevented the decrease in Tom20/DAPI, amounting to 3.2 ± 0.4 ($P < 0.01$; Figure 4D). SUL-121 also prevented the decrease in Tom20/DAPI, amounting to 2.6 ± 0.5 ($P < 0.05$; Supplementary data, Figure S1D).

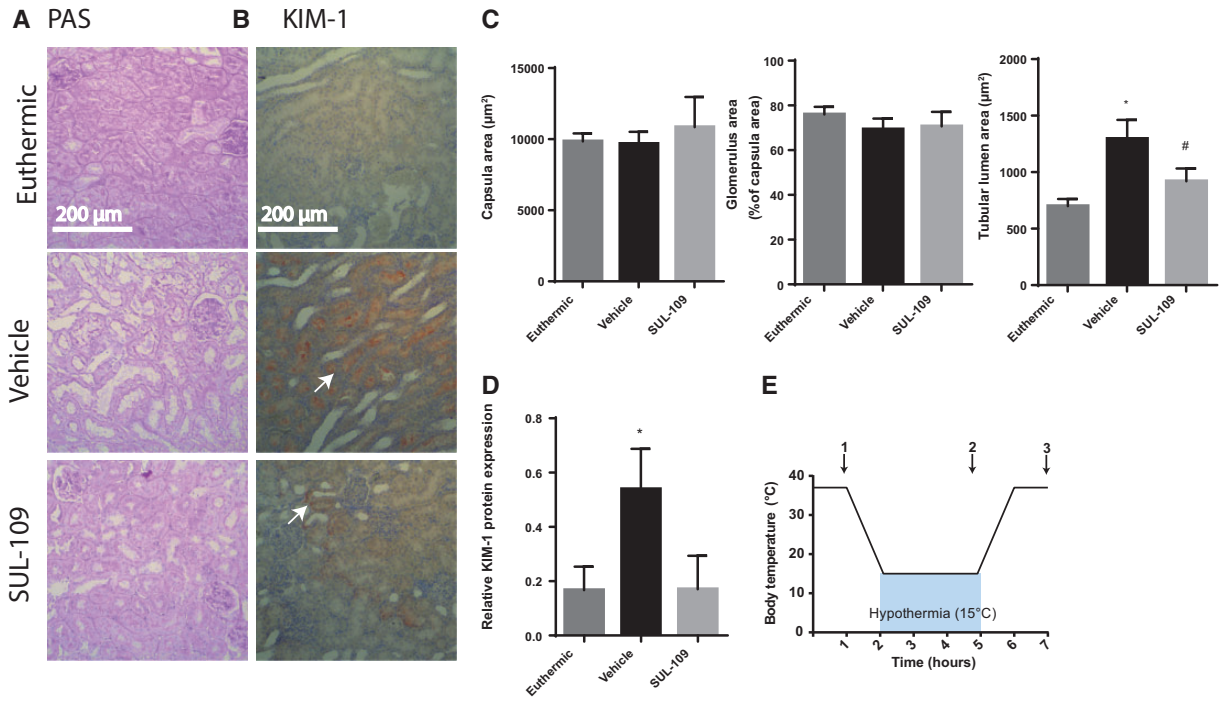

FIGURE 3: Representative sections of the kidney from the euthermic control group, the vehicle group and SUL-109 group showing PAS staining and KIM-1 immunohistochemistry (**A, B**). White arrows point to positively stained areas (brown). Graphs showing the quantification of capsule area, glomerulus area and tubular lumen area (**C**). Relative protein expression levels of KIM-1/α-tubulin in kidney homogenates (**D**). Schematic representation of the *in vivo* hypothermia/rewarming protocol (E). Starting 1 h prior to cooling, SUL-109 (135 µg/kg/h) or equal volumes of vehicle were infused throughout the experiment. Arrows indicate the moments at which samples were taken: Prior to cooling (1), prior to rewarming (2) and after rewarming (3). SUL-109 prevents hypothermia and rewarming induced kidney injury. PAS, periodic acid schiff, KIM-1, kidney injury molecule. Data are presented as means ± SD, $n = 4$ per group. *$P < 0.01$ compared to euthermic, #$P < 0.01$ versus vehicle, multiple comparison ANOVA.

In the euthermic control group, the cortical ATP levels were 5.7 ± 2.8 nmol/µg protein. In the vehicle H/R group, a decrease in ATP levels to 2.6 ± 0.6 nmol/µg was found ($P < 0.05$; Figure 4D), whereas the administration of SUL-109 prevented the loss of ATP in cortical tissue (3.7 ± 0.4 nmol/µg protein; $P < 0.05$; Figure 4D). SUL-121 also preserved cortical ATP levels (5.0 ± 2.3 nmol/µg; Supplementary data, Figure S1F). Collectively, these data suggest a rescue of mitochondrial mass and function in the 6-hydroxychromanol groups after H/R.

Oxidative stress was assessed by measuring 3-NT. Basal levels of 3-NT in euthermic control animals were detected in 33.5 ± 2.6% of the area analysed. In vehicle-treated animals (Figure 4E), 3-NT expression was increased to 72.5 ± 1.0% of the total cortical area (Figure 4E). Administration of SUL-109 decreased nitrosylated proteins to 44.0 ± 4.8% of the area ($P < 0.001$; Figure 4B, E). Administration of SUL-121 was without effect on 3-NT expression (Supplementary data, Figure S1C).

To further explore oxidative damage, we next assessed DNA damage in the kidney by measuring phosphorylated histone H2 variant (γ-H2AX) and p53 binding protein 1 (53bp1) as markers for double-strand DNA breaks (Figure 4C, Supplementary data, Figure S1E). In the euthermic control group, γ-H2AX foci were detected in 16.5 ± 11.6% of the analysed nuclei. In the vehicle group, the percentage of γ-H2AX-positive nuclei was increased to 34.2 ± 2.9%. Both SUL-109 and SUL-121 reduction of γ-H2AX-positive nuclei did not reach significance (29.5 ± 5.6% and 28.1 ± 4.2%, respectively; Supplementary data, Figure S1E). In the euthermic control group, γ-H2AX foci occurred at a frequency of 0.12 ± 0.03 per nucleus. In the vehicle group, γ-H2AX foci increased to 0.41 ± 0.04 per nucleus (Figure 4F), which was reduced by 32% in SUL-109 (0.32 ± 0.06; $P < 0.01$) and by 18% in SUL-121 (0.34 ± 0.06; $P < 0.01$). In the euthermic control group, 53bp1 co-localized in 9.1 ± 4.3% of all γ-H2AX-positive nuclei. In the H/R vehicle group, this co-localization increased to 12.8 ± 0.7% of all γ-H2AX-positive nuclei. Administration of both SUL-109 and SUL-121 decreased co-localization of 53bp1 and γ-H2AX (8.3 ± 1.4% and 5.8 ± 4.7%, respectively; $P < 0.05$). No expression of γ-H2AX and 53bp1 was observed in glomeruli (data not shown).

DISCUSSION

Here we show that 6-hydroxychromanols substituted with primary and secondary amines protect human proximal tubule cells against H/R injury *in vitro*. With the notable exception of α-tocopherol, the 6-hydroxychromanols that we tested did not differ in their efficacy (E_{max}) as they fully prevented the loss of cell viability induced by H/R. Their potency, however, denoted by EC_{50}, showed substantial variation. Based on their potency, the 6-hydroxychromanols SUL-109 and SUL-121 were selected for an *in vivo* H/R study.

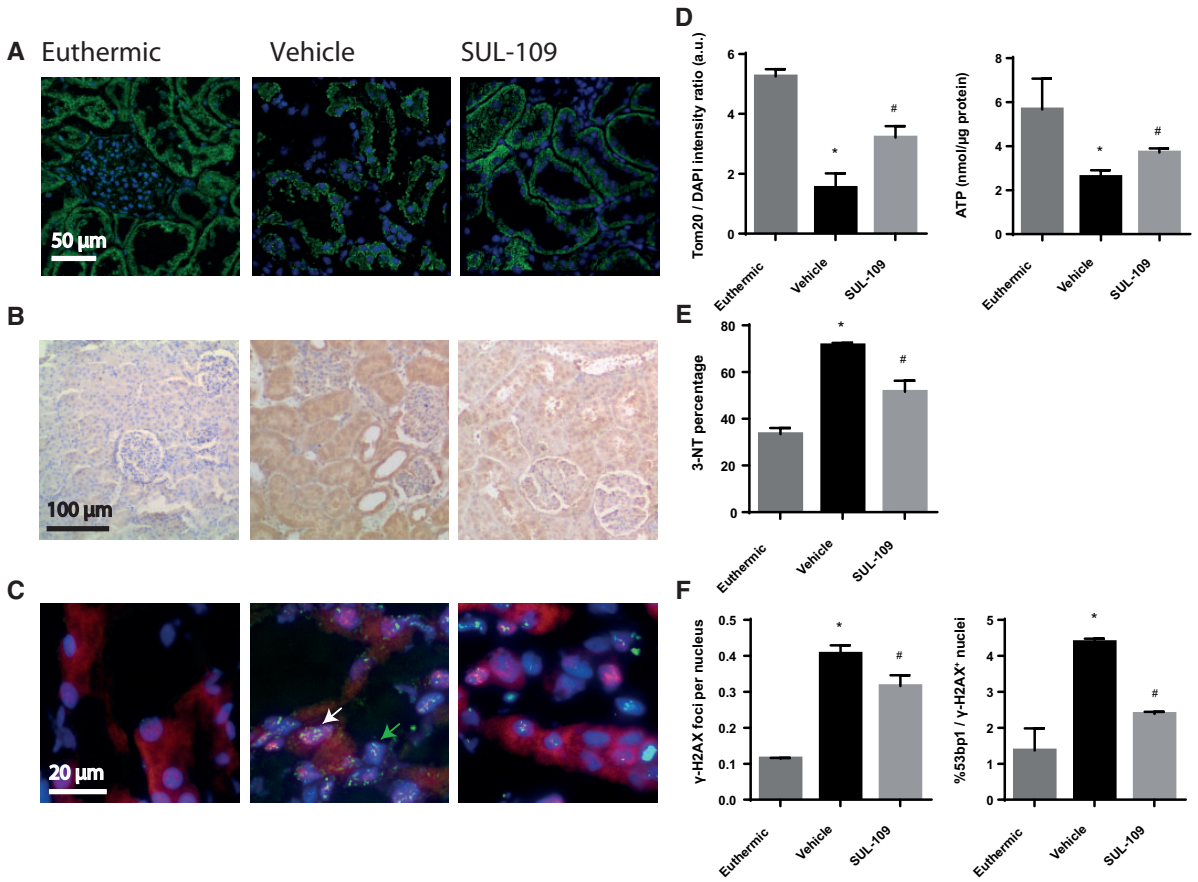

FIGURE 4: Representative sections of the kidney cortex from the euthermic control group, vehicle group and SUL-109-treated group showing (**A**) Tom20 as a marker for mitochondrial mass, (**B**) protein nitrosylation marker 3-NT in positive brown areas and (**C**) DNA damage markers γ-H2AX foci (green arrow) and co-localization with 53bp1 (white arrow). Bar graphs show (**D**) the mitochondrial mass and ATP levels, (**E**) the 3-NT-positive area and (**F**) the average number of γ-H2AX foci per nucleus and co-localization of 53bp1 with γ-H2AX. All images used from quantification were acquired in the cortex. Data are presented as mean ± SD, $n = 4$ per group. *$P < 0.01$ compared with euthermic, #$P < 0.01$ versus vehicle, multiple-comparison ANOVA.

In vivo, SUL-109 and SUL-121 protected against H/R-induced kidney injury. Both 6-hydroxychromanols ameliorated the tubular dilation and DNA damage that occurred after H/R. In addition, we observed prevention of the loss of mitochondrial mass and a safeguarding of cortical ATP levels following H/R in groups that received 6-hydroxychromanols. Together, these data indicate that SUL-109 and SUL-121 protect from H/R-induced AKI by improving mitochondrial function and limiting oxidative damage.

It should be noted that 6-hydroxychromanols may exert dual effects on oxidative damage, as they may exert chemical antioxidant effects (i.e. direct molecular interaction with an ROS) and indirect antioxidant effects (e.g. by preventing mitochondrial dysfunction, consequently decreasing ROS production, or strengthening antioxidant defences). Our results challenge a direct chemical antioxidant effect as the main beneficial effect of these 6-hydroxychromanols on H/R-induced kidney injury, but rather favour their action on mitochondria. This is substantiated by the fact that SUL-121 has a higher chemical antioxidant capacity and *in vitro* potency compared with SUL-109, yet offers comparable protection against H/R-related injury as SUL-109 at an equal dose, but fails to prevent protein nitrosylation *in vivo*. Moreover, our correlations between chemical physical characteristics and potency suggest that compound potency relates to drugability parameters, including lipophilicity and polar surface area, but not to chemical antioxidant capacity. Previous studies observing beneficial properties of chromanol-based drugs, such as the 2-methylaminochroman U83836E [30], mostly attributed this to their antioxidant properties, either chemically or indirectly. Other examples are 6-hydroxychromanol derivatives with structural similarity to SUL-109 and SUL-121, which prevent oxidative stress *in vitro* [31], and pentamethyl-6-hydroxychromanol (PMC), which prevented lipid peroxidation [32]. Interestingly, the likely mechanism of action of mitochondrial-targeted peptides that inhibit I/R injury was elucidated recently [33], showing that these peptides improve mitochondrial bioenergetics by interacting with peroxidized phospholipids, thereby safeguarding cytochrome c electron transport, whereas these peptides were previously thought to act as antioxidants [34]. Such action is in accordance with the previously reported protective effects of SUL-109 on hypothermic damage of adipose-derived stem cells through its preservation of the mitochondrial structure and membrane potential by the activation of mitochondrial

membrane complexes I and IV [22]. Further, SUL-121 was recently shown to improve the oxidative stress in diabetic *db/db* mice. In these mice, SUL-121 ameliorated renal oxidative stress, possibly by increasing renal expression of mitochondrial superoxide dismutate 2 (SOD2) [35]. Thus our results further substantiate an indirect antioxidant effect of 6-hydroxychromanols through the maintenance of mitochondrial function, since a key finding of the current study is that SUL-109 and SUL-121 increase mitochondrial mass and ATP levels in the cortex. Together, these studies indicate that the protective effect of 6-hydroxychromanols is principally dependent on their ability to maintain cellular ATP levels, decrease mitochondrial ROS production and maintain the mitochondrial antioxidative response, including SOD. Collectively, these actions preclude H/R-related renal damage and favour repair of renal injury.

H/R induced a marked loss of mitochondrial mass and ATP levels similar to those found in I/R-induced renal injury, chronic kidney disease [1, 36] and sepsis-induced renal injury [37]. These models are accompanied by systemic effects like inflammation or metabolic disposition, which makes it more difficult to study the role of mitochondrial dysfunction alone compared with the H/R model. The assessment of renal injury after 1 h of stabilization at 37°C following full rewarming from hypothermia allowed us to study the immediate effects of 6-hydroxychromanols on mitochondrial function and thus the role of mitochondrial dysfunction in early renal injury. We found that a loss of mitochondrial mass and a decrease of ATP levels after H/R-induced kidney injury preceded the increase of plasma creatinine. Even though elevated plasma creatinine levels are a hallmark of decreased kidney function, creatinine levels were only marginally elevated 1 h after rewarming from hypothermia, but more markedly after 3 h [25], suggesting that a 1 h time frame is too short for decreased kidney function to manifest itself as increased plasma creatinine levels. In addition, the virtual absence of urine production during H/R in rats precluded assessment of clinically valued parameters such as urinary albumin:creatinine ratio and fractional sodium clearance. Therefore, early assessment of renal damage in H/R may be dependent on a more rapidly responding plasma biomarker such as neutrophil gelatinase-associated lipocalin [38].

Notably, no adverse haemodynamic or toxic effects of SUL-109 and SUL-121 were observed throughout the H/R procedure. The hypothermia-associated decrease in the number of circulating WBCs and platelets and their subsequent full recovery upon rewarming are commonly reported and governed by the decrease in body temperature [39, 40]. Nevertheless, despite full normalization after rewarming, our study indicates that SUL-109 precipitated an increase in leucopenia during hypothermia. The nature of this action remains elusive, but seems unrelated to the principal mode of action of 6-hydroxychromanols, as it was absent in animals treated with SUL-121. Moreover, it remains to be established whether the amplification of leucopenic responses to cooling has any bearing on kidney injury, be it positive or negative.

LIMITATIONS OF THE CURRENT STUDY

Although the protective effects of SUL-109 and SUL-121 against hypothermia-induced tubular damage are evident, our study has some limitations. First, SUL-109-treated animals experienced a temporary decrease in pCO_2 that was restored completely upon rewarming. In absence of real-time monitoring of pO_2 and pCO_2, we determined the ventilation parameters previously in vehicle-treated animals by blood gas analysis. These ventilation parameters were used in all groups. Second, in keeping with the permit issued by the Institutional Animal Care and Use Committee, experiments were restricted to a terminal experiment under anaesthesia, which led us to investigate only the 1 h survival period to primarily establish the early effects on mitochondrial dysfunction. Future studies of animals treated with 6-hydroxychromanols might qualify for longer follow-up periods (e.g. 24–48 h) because of their protection against renal injury.

In conclusion, we show that SUL-109 and SUL-121 protect against H/R-induced kidney injury *in vivo* and might offer a promising therapeutic strategy to limit kidney injury due to maintenance of mitochondrial function.

SUPPLEMENTARY DATA

Supplementary data are available at ndt online.

ACKNOWLEDGEMENTS

Imaging was performed at the University Medical Center Groningen Imaging Center, which is supported by The Netherlands Organization for Health Research and Development (40-00506-98-9021), and we thank K. Sjollema for technical support during imaging. We acknowledge K. C. van Zomeren (Department of Neuroscience, University Medical Center) for his support and discussion during the development of image analysis methods. We thank L.A. Brouwer (Department Pathology and Medical Biology, University Medical Center Groningen, The Netherlands) for technical support and enabling image analysis. A. Heeres (Syncom, Groningen, The Netherlands) offered expert support regarding development of the compound library and physiochemical analyses.

FUNDING

Development of the SUL compounds was financially supported by grants from the Innovative Action Program Groningen 2010–13 (IAG3 to A.C.v.d.G.) and the 'Samenwerkingsverband Noord Nederland (SNN)' EFRO Tender Valorization (http://www.snn.eu; to A.C.v.d.G.). H.B., G.K. and R.H.H. are supported by the Groningen University Institute for Drug Exploration and G.K. is supported by Innovational Research Incentive grants from the Netherlands Organization for Health Research and Development (916.11.022 and 917.16.466). Funding bodies had no role in study design, data collection, data analysis and interpretation, the decision to publish or preparation of the manuscript.

AUTHORS' CONTRIBUTIONS

P.C.V., R.H.H. and G.K. drafted the manuscript. R.H.H., H.B., G.K. and A.C.v.d.G. designed the experiments. P.C.V. and M.R. performed the experiments and data analysis and prepared the figures. G.K. performed data analysis and prepared the figures. E.V., H.B., M.C.H. and M.G. performed animal experiments and data analysis. G.K., R.H.H. and A.C.v.d.G. proofread the manuscript. H.B., G.K and R.H.H. revised the article.

CONFLICT OF INTEREST STATEMENT

The results presented in this article have not been published previously in whole or part. No part of the manuscript has been published before, nor is any part of it under consideration for publication at another journal. P.C.V. is chief of operations, A.C.v.d.G. is a stockholder and the chief executive officer and G.K. is the chief scientific officer at Sulfateq (Groningen, The Netherlands), a company that owns patents on SUL-109 and SUL-121 and produces and markets these and similar compounds. R.H.H. and M.R. report personal fees from Sulfateq during the conduct of the study. A.C.v.d.G. reports personal fees from Sulfateq during the conduct of the study and has a patent (WO2014098586 A1) pending.

REFERENCES

1. Che R, Yuan Y, Huang S *et al.* Mitochondrial dysfunction in the pathophysiology of renal diseases. *Am J Physiol Renal Physiol* 2014; 306: F367–F378
2. Funk JA, Schnellmann RG. Persistent disruption of mitochondrial homeostasis after acute kidney injury. *Am J Physiol Renal Physiol* 2012; 302: F853–F864
3. De Rosa S, Antonelli M, Ronco C. Hypothermia and kidney: a focus on ischaemia–reperfusion injury. *Nephrol Dial Transplant* 2017; 32: 241–247
4. Sato T, Tauchi H. Age changes of mitochondria of rat kidney. *Mech Ageing Dev* 1982; 20: 111–126
5. Visarius TM, Putt DA, Schare JM *et al.* Pathways of glutathione metabolism and transport in isolated proximal tubular cells from rat kidney. *Biochem Pharmacol* 1996; 52: 259–272
6. Hall AM, Unwin RJ, Parker N *et al.* Multiphoton imaging reveals differences in mitochondrial function between nephron segments. *J Am Soc Nephrol* 2009; 20: 1293–1302
7. Brooks C, Wei Q, Cho SG *et al.* Regulation of mitochondrial dynamics in acute kidney injury in cell culture and rodent models. *J Clin Invest* 2009; 119: 1275–1285
8. Ishimoto Y, Inagi R. Mitochondria: a therapeutic target in acute kidney injury. *Nephrol Dial Transplant* 2016; 31: 1062–1069
9. Dugbartey GJ, Hardenberg MC, Kok WF *et al.* Renal mitochondrial response to low temperature in non-hibernating and hibernating species. *Antioxid Redox Signal* 2017; 27: 599–617
10. Dugbartey GJ, Bouma HR, Saha MN *et al.* Hibernation-like state for transplantable organs: is hydrogen sulfide therapy the future of organ preservation? *Antioxid Redox Signal* 2017; doi:10.1089/ars.2017.7127
11. Heyman SN, Evans RG, Rosen S *et al.* Cellular adaptive changes in AKI: mitigating renal hypoxic injury. *Nephrol Dial Transplant* 2012; 27: 1721–1728
12. Boutilier RG. Mechanisms of cell survival in hypoxia and hypothermia. *J Exp Biol* 2001; 204: 3171–3181
13. Alva N, Palomeque J, Carbonell T. Oxidative stress and antioxidant activity in hypothermia and rewarming: can rons modulate the beneficial effects of therapeutic hypothermia? *Oxid Med Cell Longev* 2013; 2013: 1–10
14. Andreyev A, Fiskum G. Calcium induced release of mitochondrial cytochrome c by different mechanisms selective for brain versus liver. *Cell Death Differ* 1999; 6: 825–832
15. Devarajan P. Update on mechanisms of ischemic acute kidney injury alterations in morphology. *J Am Soc Nephrol* 2006; 17: 1503–1520
16. Devarajan P. Cellular and molecular derangements in acute tubular necrosis. *Curr Opin Pediatr* 2005; 17: 193–199
17. Rhoden EL, Pereira-Lima L, Telöken C *et al.* Beneficial effect of alpha-tocopherol in renal ischemia-reperfusion in rats. *Jpn J Pharmacol* 2001; 87: 164–166
18. Avunduk MC, Yurdakul T, Erdemli E *et al.* Prevention of renal damage by alpha Tocopherol in ischemia and reperfusion models of rats. *Urol Res* 2003; 31: 280–285
19. Wongmekiat O, Thamprasert K, Lumlertgul D. Renoprotective effect of TROLOX against ischaemia-reperfusion injury in rats. *Clin Exp Pharmacol Physiol* 2007; 34: 753–759
20. Dagenais GR, Marchioli R, Yusuf S *et al.* Beta-carotene, vitamin C, and vitamin E and cardiovascular diseases. *Curr Cardiol Rep* 2000; 2: 293–299
21. Vivekananthan DP, Penn MS, Sapp SK *et al.* Use of antioxidant vitamins for the prevention of cardiovascular disease: meta-analysis of randomised trials. *Lancet* 2003; 361: 2017–2023
22. Hajmousa G, Vogelaar P, Brouwer LA *et al.* The 6-chromanol derivate SUL-109 enables prolonged hypothermic storage of adipose tissue-derived stem cells. *Biomaterials* 2017; 119: 43–52
23. Dankers PYW, Boomker JM, Huizinga-van der Vlag A *et al.* The use of fibrous, supramolecular membranes and human tubular cells for renal epithelial tissue engineering: towards a suitable membrane for a bioartificial kidney. *Macromol Biosci* 2010; 10: 1345–1354
24. Dankers PYW, Boomker JM, Huizinga-van der Vlag A *et al.* Bioengineering of living renal membranes consisting of hierarchical, bioactive supramolecular meshes and human tubular cells. *Biomaterials* 2011; 32: 723–733
25. Dugbartey GJ, Talaei F, Houwertjes MC *et al.* Dopamine treatment attenuates acute kidney injury in a rat model of deep hypothermia and rewarming—the role of renal H_2S-producing enzymes. *Eur J Pharmacol* 2015; 769: 225–233
26. Schindelin J, Rueden CT, Hiner MC *et al.* The ImageJ ecosystem: an open platform for biomedical image analysis. *Mol Reprod Dev* 2015; 82: 518–529
27. Kotyk T, Dey N, Ashour AS *et al.* Measurement of glomerulus diameter and Bowman's space width of renal albino rats. *Comput Methods Programs Biomed* 2016; 126: 143–153
28. Chida J, Yamane K, Takei T *et al.* An efficient extraction method for quantitation of adenosine triphosphate in mammalian tissues and cells. *Anal Chim Acta* 2012; 727: 8–12
29. Motulsky HJ, Brown RE. Detecting outliers when fitting data with nonlinear regression – a new method based on robust nonlinear regression and the false discovery rate. *BMC Bioinformatics* 2006; 7: 123
30. De Vecchi E, Lubatti L, Beretta C *et al.* Protection from renal ischemia-reperfusion injury by the 2-methylaminochroman U83836E. *Kidney Int* 1998; 54: 857–863
31. Blanchet L, Smeitink JAM, van Emst-de Vries SE *et al.* Quantifying small molecule phenotypic effects using mitochondrial morpho-functional fingerprinting and machine learning. *Sci Rep* 2015; 5: 8035
32. Samhan-Arias AK, Tyurina YY, Kagan VE. Lipid antioxidants: free radical scavenging versus regulation of enzymatic lipid peroxidation. *J Clin Biochem Nutr* 2011; 48: 91–95
33. Birk AV, Liu S, Soong Y *et al.* The mitochondrial-targeted compound SS-31 re-energizes ischemic mitochondria by interacting with cardiolipin. *J Am Soc Nephrol* 2013; 24: 1250–1261
34. Zhao K, Zhao G-M, Wu D *et al.* Cell-permeable peptide antioxidants targeted to inner mitochondrial membrane inhibit mitochondrial swelling, oxidative cell death, and reperfusion injury. *J Biol Chem* 2004; 279: 34682–34690
35. Lambooy SPH, Bidadkosh A, Nakladal D *et al.* The novel compound sul-121 preserves endothelial function and inhibits progression of kidney damage in type 2 diabetes mellitus in mice. *Sci Rep* 2017; 7: 11165
36. Ma Z, Wei Q, Dong G *et al.* DNA damage response in renal ischemia-reperfusion and ATP-depletion injury of renal tubular cells. *Biochim Biophys Acta* 2014; 1842: 1088–1096
37. Lowes DA, Webster NR, Murphy MP *et al.* Antioxidants that protect mitochondria reduce interleukin-6 and oxidative stress, improve mitochondrial function, and reduce biochemical markers of organ dysfunction in a rat model of acute sepsis. *Br J Anaesth* 2013; 110: 472–480

38. Alge JL, Arthur JM. Biomarkers of AKI: a review of mechanistic relevance and potential therapeutic implications. *Clin J Am Soc Nephrol* 2015; 10: 147–155
39. Shenaq SA, Yawn DH, Saleem A *et al*. Effect of profound hypothermia on leukocytes and platelets. *Ann Clin Lab Sci* 1986; 16: 130–133
40. de Vrij EL, Vogelaar PC, Goris M *et al*. Platelet dynamics during natural and pharmacologically induced torpor and forced hypothermia. *PLoS One* 2014; 9: e93218

Received: 19.9.2017; Editorial decision: 3.3.2018